

## Shape transitions in excited states of two-electron quantum dots in a magnetic field

This article has been downloaded from IOPscience. Please scroll down to see the full text article.

2012 J. Phys. B: At. Mol. Opt. Phys. 45 205503

(<http://iopscience.iop.org/0953-4075/45/20/205503>)

View [the table of contents for this issue](#), or go to the [journal homepage](#) for more

Download details:

IP Address: 150.214.103.186

The article was downloaded on 19/09/2012 at 15:21

Please note that [terms and conditions apply](#).

# Shape transitions in excited states of two-electron quantum dots in a magnetic field

R G Nazmitdinov<sup>1,2</sup>, N S Simonović<sup>3</sup>, A R Plastino<sup>4,5</sup> and A V Chizhov<sup>2</sup>

<sup>1</sup> Departament de Física, Universitat de les Illes Balears, E-07122 Palma de Mallorca, Spain

<sup>2</sup> Bogoliubov Laboratory of Theoretical Physics, Joint Institute for Nuclear Research, 141980 Dubna, Russia

<sup>3</sup> Institute of Physics, University of Belgrade, PO Box 57, 11001 Belgrade, Serbia

<sup>4</sup> Instituto Carlos I de Física Teórica y Computacional, Universidad de Granada, E-18071 Granada, Spain

<sup>5</sup> National University La Plata, UNLP-CREG-CONICET, CC 727, La Plata 1900, Argentina

E-mail: arplastino@ugr.es

Received 30 May 2012

Published 18 September 2012

Online at [stacks.iop.org/JPhysB/45/205503](http://stacks.iop.org/JPhysB/45/205503)

## Abstract

We use entanglement to study shape transitions in two-electron axially symmetric parabolic quantum dots in a perpendicular magnetic field. At a specific magnetic field value the dot attains a spherical symmetry. The transition from the axial to the spherical symmetry manifests itself as a drastic change of the entanglement of the lowest state with zero angular momentum projection. While the electrons in such a state are always localized in the plane ( $x - y$ ) before the transition point, after this point they become localized in the vertical direction.

Besides its well-known role in the implementation of quantum information technologies, entanglement is nowadays also regarded as an essential ingredient for the analysis and characterization of quantum many-body systems [1]. This latter point of view is currently the focus of an increasing research activity, establishing new connections between quantum information theory and other branches of physics, such as atomic, molecular and condensed matter physics [1–15]. In particular, there is a growing interest in using quantum entanglement measures for the study of quantum correlations in topologically ordered systems [16]. The analysis of these systems is a highly non-trivial task due to the absence of the order parameter. The main stream of such an analysis is focused on quantum-phase transitions in many-particle one-dimensional systems [17]. It is noteworthy that various phases are exhibited in quantum dots (QDs) at different strengths of the applied perpendicular magnetic field [18]. Two-electron QDs being realistic tractable nontrivial systems are, in particular, attractive because their eigenstates can be obtained very accurately, or in some cases, exactly (cf [19, 20]). The objective of this paper is to demonstrate that quantum entanglement can be used to trace a shape-phase transition in excited states of two interacting electrons confined in a three-dimensional (3D) QD in a magnetic field.

Our analysis is carried out by means of the exact diagonalization of the Hamiltonian:

$$H = \sum_{j=1}^2 \left[ \frac{1}{2m^*} \left( \mathbf{p}_j - \frac{e}{c} \mathbf{A}_j \right)^2 + U(\mathbf{r}_j) \right] + \frac{k}{|\mathbf{r}_1 - \mathbf{r}_2|} + H_{\text{spin}}. \quad (1)$$

Here  $k = e^2/4\pi\epsilon_0\epsilon_r$  and  $H_{\text{spin}} = g^*\mu_B(\mathbf{s}_1 + \mathbf{s}_2) \cdot \mathbf{B}$  describes the Zeeman term, where  $\mu_B = e\hbar/2m_e c$  is the Bohr magneton. As an example, we will use the effective mass  $m^* = 0.067m_e$ , the relative dielectric constant  $\epsilon_r = 12$  and the effective Landé factor  $g^* = -0.44$  (bulk GaAs values). For the perpendicular magnetic field, we choose the vector potential with gauge  $\mathbf{A} = \frac{1}{2}\mathbf{B} \times \mathbf{r} = \frac{1}{2}B(-y, x, 0)$ . The confining potential is approximated by a 3D axially symmetric harmonic oscillator  $U(\mathbf{r}) = m^*[\omega_0^2(x^2 + y^2) + \omega_z^2 z^2]/2$ , where  $\hbar\omega_z$  and  $\hbar\omega_0$  are the energy scales of confinement in the  $z$ -direction and in the  $xy$ -plane, respectively.

By introducing the centre of mass (CM) and relative coordinates:  $\mathbf{R} = \frac{1}{2}(\mathbf{r}_1 + \mathbf{r}_2)$  and  $\mathbf{r}_{12} = \mathbf{r}_1 - \mathbf{r}_2$ , the Hamiltonian (1), in agreement with the Kohn theorem [21], separates into the CM and relative-motion terms  $H = H_{\text{CM}} + H_{\text{rel}}$  (see details in [20]). The CM term is described by the oscillator Hamiltonian with the mass  $\mathcal{M} = 2m^*$  and frequencies of

the one-particle confining potential  $U$ . The Hamiltonian for relative motion in cylindrical coordinates takes the form

$$H_{\text{rel}} = \frac{1}{2\mu} \left( p_{\rho_{12}}^2 + \frac{l_z^2}{\rho_{12}^2} + p_{\varphi_{12}}^2 \right) + \frac{\mu}{2} (\Omega^2 \rho_{12}^2 + \omega_z^2 z_{12}^2) + \frac{k}{r_{12}} - \omega_L l_z, \quad (2)$$

where  $\mu = m^*/2$  is the reduced mass,  $l_z (\rightarrow -i\hbar\partial/\partial\varphi_{12})$  is the projection of angular momentum for relative motion and  $\rho_{12}^2 = (x_{12}^2 + y_{12}^2)^{1/2}$ ,  $\varphi_{12} = \arctan(y_{12}/x_{12})$  and  $r_{12} = (\rho_{12}^2 + z_{12}^2)^{1/2}$ . Here,  $\omega_L = eB/2m^*c$  is the Larmor frequency, and the effective lateral confinement frequency  $\Omega = (\omega_L^2 + \omega_0^2)^{1/2}$  depends through  $\omega_L$  on the magnetic field.

The total two-electron wavefunction  $\Psi(\mathbf{r}_1, \mathbf{r}_2) = \psi(\mathbf{r}_1, \mathbf{r}_2)\chi(\sigma_1, \sigma_2)$  is a product of the orbital  $\psi(\mathbf{r}_1, \mathbf{r}_2)$  and spin  $\chi(\sigma_1, \sigma_2)$  wavefunctions. Due to the Kohn theorem, the orbital wavefunction is factorized as a product of the CM and the relative motion wavefunctions

$$\psi(\mathbf{r}_1, \mathbf{r}_2) = \psi_{\text{CM}}(\mathbf{R}) \psi_{\text{rel}}(\mathbf{r}_{12}). \quad (3)$$

According to the Pauli principle, the orbital wavefunction must be symmetric (or, equivalently,  $\psi_{\text{rel}}(\mathbf{r}_{12})$  must be even) for the antisymmetric (singlet:  $S = M_S = 0$ ) spin state, and it must be antisymmetric ( $\psi_{\text{rel}}(\mathbf{r}_{12})$  must be odd) for the symmetric (triplet:  $S = 1, M_S = 0, \pm 1$ ) spin states. Thus, for the relative motion the parity of  $\psi_{\text{rel}}(\mathbf{r}_{12})$  is a good quantum number as well as the magnetic quantum number  $m$ , since  $l_z$  is the integral of motion.

The CM eigenfunction is a product of the Fock–Darwin state (the eigenstate of electron in an isotropic 2D harmonic oscillator potential in a perpendicular magnetic field) [22] in the  $(X, Y)$ -plane and the oscillator function in the  $Z$ -direction (both sets for a particle of mass  $\mathcal{M}$ ). In this paper, we consider the lowest CM eigenstate which has the form  $\psi_{\text{CM}}(\mathbf{R}) = \psi_{\text{CM}}^{(xy)}(X, Y) \psi_{\text{CM}}^{(z)}(Z)$ , where  $\psi_{\text{CM}}^{(xy)}(X, Y) = \sqrt{2\bar{\Omega}/\pi} e^{-\bar{\Omega}(X^2+Y^2)}$  and  $\psi_{\text{CM}}^{(z)}(Z) = (2\bar{\omega}_z/\pi)^{1/4} e^{-\bar{\omega}_z Z^2}$  (i.e. zero-principle quantum numbers), with  $\bar{\Omega} = m^*\Omega/\hbar$  and  $\bar{\omega}_z = m^*\omega_z/\hbar$ .

Since the Coulomb interaction mixes the eigenstates of non-interacting electrons, the eigenfunctions of the Hamiltonian for relative motion (2) are expanded in the basis of the Fock–Darwin states  $\Phi_{n,m}(\rho_{12}, \varphi_{12})$  and oscillator functions in the  $z_{12}$ -direction  $\phi_{n_z}(z_{12})$  (for a particle of mass  $\mu$ ), i.e.

$$\psi_{\text{rel}}(\mathbf{r}_{12}) = \sum_{n,n_z} c_{n,n_z}^{(m)} \Phi_{n,m}(\rho_{12}, \varphi_{12}) \phi_{n_z}(z_{12}). \quad (4)$$

The coefficients  $c_{n,n_z}^{(m)}$  can be determined by diagonalizing the Hamiltonian (2) in the same basis. Evidently, in numerical analysis the basis is restricted to a finite set  $\{\Phi_{n,m} \phi_{n_z} | n = 0, \dots, n_{\text{max}}; n_z = 0, \dots, n_z^{\text{max}}\}$ . It must be, however, large enough to provide a good convergence for the numerical results. Since the function  $\psi_{\text{rel}}(\mathbf{r}_{12})$  has a definite parity and the parity of the functions  $\Phi_{n,m} \phi_{n_z}$  is  $(-1)^{m+n_z}$ , the index  $n_z$  in expansion (4) takes either even or odd values.

For non-interacting electrons ( $k = 0$ ) the eigenfunctions  $\psi_{\text{rel}}$  are simply the basis functions  $\Phi_{n,m} \phi_{n_z}$ , and, therefore, the ground state is described by the wavefunction  $\psi_{\text{rel}} = \Phi_{0,0} \phi_0$ . When two interacting electrons move in the external field

created by the confining potential and the applied, varying steadily, magnetic field, the quantum number  $m$  of the ground state (in the form (4)) evolves from zero to higher values as the magnetic field strength increases. It results in the well-known singlet–triplet transitions [23]. Namely for a given  $m$  the dominant term in expansion (4) will be  $\Phi_{0,m} \phi_0$  ( $\Rightarrow$  all  $n_z$  are even) and the parity of the ground state is  $(-1)^m$ , which determines the total spin to be  $S = \frac{1}{2}[1 - (-1)^m]$ . Note that the quantum number  $M_S$  associated with the spin wavefunction evolves as follows: for even  $m$  the total spin  $S = 0$  and, thus,  $M_S = 0$ ; for odd  $m$  the total spin  $S = 1$  and  $M_S$  can be  $-1, 0$  or  $1$ . The Zeeman splitting (with  $g^* < 0$ ) will lower the energy of the  $M_S = 1$  component of the triplet states while leaving the singlet states unchanged. As a consequence, the ground state will be characterized by  $M_S = S$ . With the increasing magnetic field the intervals of the triplet states will increase at the cost of the singlet ones, and eventually, the singlet ground states will be totally suppressed. The increase of the magnetic field leads to the formation of a ring and a torus of maximal density in 2D and 3D densities, respectively (see figure 4 in [24]).

At the value  $\omega_L^{\text{sph}} = (\omega_z^2 - \omega_0^2)^{1/2}$ , the magnetic field gives rise to the *spherical symmetry* ( $\omega_z/\Omega = 1$ ) (with  $\omega_z > \omega_0$ ) in the *axially symmetric* two-electron QD [25, 26]. This phenomenon was also recognized in the results for many interacting electrons in self-assembled QDs [27]. In the latter case, it was interpreted as an approximate symmetry that had survived from the non-interacting case due to the dominance of the confinement energy over a relatively small Coulomb interaction energy. However, the symmetry is not approximate but *exact* even for strongly interacting electrons, because the radial electron–electron repulsion does not break the rotational symmetry. A natural question arises: how to detect such a transition looking on the density distribution only? A related question is: if such a transition occurs, what are the concomitant structural changes?

To this end, we employ the entanglement measure based on the linear entropy of reduced density matrices (cf [28]):

$$\mathcal{E} = 1 - 2 \text{Tr}[\rho_r^{(\text{orb})2}] \text{Tr}[\rho_r^{(\text{spin})2}], \quad (5)$$

where  $\rho_r^{(\text{orb})}$  and  $\rho_r^{(\text{spin})}$  are the single-particle-reduced density matrices in the orbital and spin spaces, respectively. This measure is quite popular for the analysis of the entanglement of two-fermion systems, in particular, two electrons confined in the parabolic potential in the absence of the magnetic field [10, 15, 29]. Note that the measure (5) vanishes when the global (pure) state describing the two electrons can be expressed as one single Slater determinant.

The trace  $\text{Tr}[\rho_r^{(\text{spin})2}]$  of the two-electron spin states with a definite symmetry  $\chi_{S,M_S}$  has two values: (i)  $1/2$  if  $M_S = 0$  (anti-parallel spins of two electrons); (ii)  $1$  if  $M_S = \pm 1$  (parallel spins). The condition  $M_S = S = \frac{1}{2}[1 - (-1)^m]$  yields

$$\text{Tr}[\rho_r^{(\text{spin})2}] = \frac{1}{2}(1 + |M_S|) = \frac{3 - (-1)^m}{4}. \quad (6)$$

The trace of the orbital part  $\text{Tr}[\rho_r^{(\text{orb})2}]$

$$\text{Tr}[\rho_r^{(\text{orb})2}] = \int d\mathbf{r}_1 d\mathbf{r}'_1 d\mathbf{r}_2 d\mathbf{r}'_2 \psi(\mathbf{r}_1, \mathbf{r}_2) \psi^*(\mathbf{r}'_1, \mathbf{r}_2) \psi^*(\mathbf{r}_1, \mathbf{r}'_2) \psi(\mathbf{r}'_1, \mathbf{r}_2) \quad (7)$$

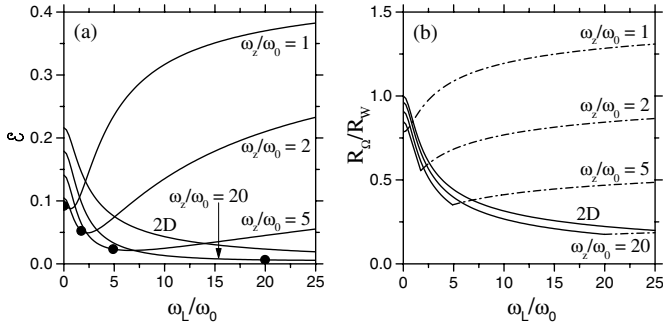


**Figure 1.** (a) Entanglement of the lowest state with  $m = 0$  at  $R_W = 2$  and various ratios  $\omega_z/\omega_0$  as functions of the parameter  $\omega_L/\omega_0$ . The circles denote the values of  $\omega_L/\omega_0$  when QDs with given ratios  $\omega_z/\omega_0$  become spherically symmetric. (b) The relative strength of the Coulomb interaction  $R_\Omega^{(2D)}/R_W$  (solid line) and  $R_\Omega^{(1D)}/R_W$  (dash-dotted line) for the lowest state with  $m = 0$  at various ratios  $\omega_z/\omega_0$  as functions of the parameter  $\omega_L/\omega_0$ .

is more involved. Indeed, in virtue of equations (3) and (4), one obtains

$$\text{Tr}[\rho_r^{(\text{orb})2}] = \sum_{n_1=0}^{n_{\max}} \sum_{n_2=0}^{n_{\max}} \sum_{n_3=0}^{n_{\max}} \sum_{n_4=0}^{n_{\max}} \sum_{n_{z_1}=0}^{n_z^{\max}} \sum_{n_{z_2}=0}^{n_z^{\max}} \sum_{n_{z_3}=0}^{n_z^{\max}} \sum_{n_{z_4}=0}^{n_z^{\max}} c_{n_1, n_{z_1}}^{(m)} c_{n_2, n_{z_2}}^{(m)} c_{n_3, n_{z_3}}^{(m)} c_{n_4, n_{z_4}}^{(m)} I(n_1, n_2, n_3, n_4; m) J(n_{z_1}, n_{z_2}, n_{z_3}, n_{z_4}), \quad (8)$$

where

$$I(n_1, n_2, n_3, n_4; m) = \int d\mathbf{r}_1 d\mathbf{r}'_1 d\mathbf{r}_2 d\mathbf{r}'_2 \psi_{\text{CM}}^{(xy)}\left(\frac{\mathbf{r}_1+\mathbf{r}_2}{2}\right) \psi_{\text{CM}}^{(xy)*}\left(\frac{\mathbf{r}'_1+\mathbf{r}'_2}{2}\right) \psi_{\text{CM}}^{(xy)*}\left(\frac{\mathbf{r}_1+\mathbf{r}'_1}{2}\right) \psi_{\text{CM}}^{(xy)}\left(\frac{\mathbf{r}'_1+\mathbf{r}'_2}{2}\right) \Phi_{n_1, m}(\mathbf{r}_1 - \mathbf{r}_2) \Phi_{n_2, m}^*(\mathbf{r}'_1 - \mathbf{r}_2) \Phi_{n_3, m}^*(\mathbf{r}_1 - \mathbf{r}'_2) \Phi_{n_4, m}(\mathbf{r}'_1 - \mathbf{r}'_2) \quad (9)$$

(here  $\mathbf{r}_i$  are vectors in the  $xy$ -plane) and

$$J(n_{z_1}, n_{z_2}, n_{z_3}, n_{z_4}) = \int dz_1 dz'_1 dz_2 dz'_2 \psi_{\text{CM}}^{(z)}\left(\frac{z_1+z_2}{2}\right) \psi_{\text{CM}}^{(z)*}\left(\frac{z'_1+z'_2}{2}\right) \psi_{\text{CM}}^{(z)*}\left(\frac{z_1+z'_1}{2}\right) \psi_{\text{CM}}^{(z)}\left(\frac{z'_1+z'_2}{2}\right) \phi_{n_{z_1}}(z_1 - z_2) \phi_{n_{z_2}}^*(z'_1 - z_2) \phi_{n_{z_3}}^*(z_1 - z'_2) \phi_{n_{z_4}}(z'_1 - z'_2). \quad (10)$$

The magnetic field dependence of the entanglement  $\mathcal{E}$  naturally occurs via inherent variability of the expansion coefficients. The values of the  $I$  and  $J$  integrals for any choice of indices can be determined analytically, which simplifies the numerical calculations.

For our analysis, it is convenient to use the so-called Wigner parameter  $R_W = (k/l_0)/\hbar\omega_0 = l_0/a^*$ , a measure of the Coulomb interaction strength relative to the confinement strength (cf [20]). Here,  $l_0 = \sqrt{\hbar/m^*\omega_0}$  is the oscillator length and  $a^* = \hbar^2/km^*$  is the effective Bohr radius. For our choice of the parameters (GaAs) and for the confinement frequency  $\hbar\omega_0 \approx 2.8$  MeV we have  $R_W \approx 2$ . The numerical analysis demonstrates a good convergence for the basis with  $n_{\max} = n_z^{\max} = 4$ .

In the absence of the magnetic field ( $B = 0$ ), the entanglement decreases if the ratio  $\omega_z/\omega_0$  decreases from  $\infty$  (2D model) to 1 (spherically symmetric 3D model); see figure 1(a) at  $\omega_L/\omega_0 = 0$ . This effect could be explained by introducing the effective charge  $k_{\text{eff}}$  [25, 30] which determines

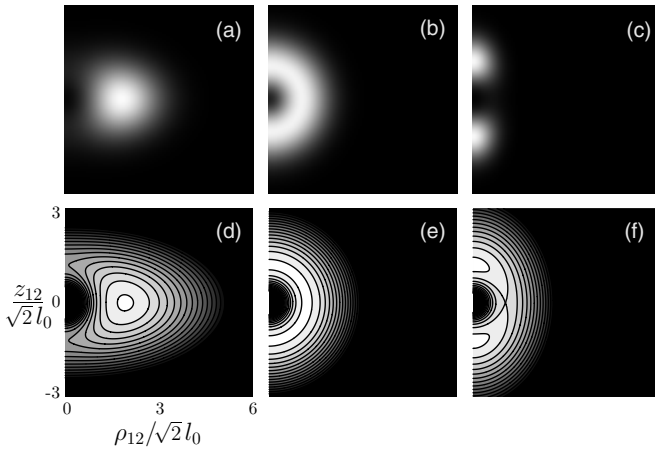
the effective electron–electron interaction  $V_C = k_{\text{eff}}/\rho_{12}$  in the QD. In the 3D dot the electrons can avoid each other more effectively than in the 2D one. Therefore, the Coulomb interaction has a smaller effect on the 3D spectrum (the ratio  $k_{\text{eff}}/k \sim 0.5$ ) in contrast to the 2D case when  $k_{\text{eff}}/k = 1$ . Thus, a decrease of the ratio  $\omega_z/\omega_0$  yields an analogous effect as the reduction of the electron–electron interaction.

Figure 1(a) shows the entanglement measure  $\mathcal{E}$  of the lowest angular momentum state  $m = 0$  as a function of the magnetic field (the parameter  $\omega_L/\omega_0$ ) at a fixed value of  $R_W$  and for different ratios  $\omega_z/\omega_0$ . In the 2D case, the entanglement decreases monotonically with the increase of the magnetic field. The constant electron–electron interaction becomes relatively weaker, since the effective lateral confinement ( $\hbar\Omega$ ) increases with the magnetic field. If we introduce the characteristic length of the effective confinement  $l_\Omega = \sqrt{\hbar/m^*\Omega}$ , the parameter  $R_\Omega = l_\Omega/a^*$  (which is equal  $R_W$  at  $B = 0$ ) determines the relative strength of Coulomb interaction at a given effective confinement. Evidently,  $R_\Omega$  decreases with the increase of the magnetic field  $B$  (see figure 1(b), the line labelled ‘2D’). In the 3D case, however, the entanglement decreases until  $\omega_L = \omega_L^{\text{sph}}$ , when the spherical symmetry occurs. After this point the entanglement starts to increase (see figure 1(a)).

This behaviour can be explained by the influence of the magnetic field on the effective strength  $R_\Omega$ , which is twofold here. Indeed, in the 3D case the magnetic field affects the effective charge as well as the effective confinement. For the quasi-2D system of electrons ( $\Omega \ll \omega_z$ ), the effective charge is  $k_{\text{eff}}^{(2D)} = \langle \rho_{12} V_C \rangle$  (see equation (18) in [30]), where  $V_C = k/\sqrt{\rho_{12}^2 + z_{12}^2}$  is the full 3D Coulomb interaction. The mean value  $\langle \rho_{12} V_C \rangle$  is calculated by means of the eigenstates of  $H_{\text{rel}}$  in the approximation of non-interacting electrons. Here, the eigenstate is  $\Phi_{0, m} \phi_0$  (for explicit expressions see equations (19) and (20) in [30]). Thus, for the quasi-2D case the parameter  $R_\Omega^{(2D)} = (m^*/\hbar^3 \Omega)^{1/2} k_{\text{eff}}^{(2D)}$  can be used as a measure for the relative strength of the Coulomb interaction.

For  $\Omega \gg \omega_z$  (very strong magnetic field), the electrons are pushed laterally towards the dot’s centre. The magnetic field, however, does not affect the vertical confinement. As a consequence, the electrons practically can move only in the  $z$ -direction and the QD becomes a quasi-1D system. In this case, a measure for the relative strength of the Coulomb interaction can be defined as  $R_\Omega^{(1D)} = (m^*/\hbar^3 \omega_z)^{1/2} k_{\text{eff}}^{(1D)}$ , where the effective charge for a quasi-1D system is  $k_{\text{eff}}^{(1D)} = \langle |z_{12}| V_C \rangle$ . It can be shown that for the lowest state with  $m = 0$  one obtains  $k_{\text{eff}}^{(1D)}/k = (1 + \sqrt{\omega_z/\Omega})^{-1}$ .

The quantities  $R_\Omega^{(2D)}$  and  $R_\Omega^{(1D)}$  for the lowest state with  $m = 0$ , as functions of the parameter  $\omega_L/\omega_0$  (in the domains  $0 < \omega_L < \omega_L^{\text{sph}}$  and  $\omega_L > \omega_L^{\text{sph}}$ , respectively), are shown in figure 1(b) for different ratios  $\omega_z/\omega_0$ . One observes that the effective strength  $R_\Omega^{(2D)}$  decreases with the increase of the magnetic field for different ratios  $\omega_z/\omega_0$ , similar to the 2D case. The oppositely ordered confinement  $\Omega^{(1D)}$  (which is not defined for the 2D case) increases with  $\omega_L$  and, therefore, the effective strength  $R_\Omega^{(1D)}$  increases as well. In order to match  $R_\Omega^{(1D)} = R_\Omega^{(2D)}$  at  $\omega_L = \omega_L^{\text{sph}}$  (i.e. when  $\Omega = \omega_z$ ), the strength  $R_\Omega^{(1D)}$  is scaled by the factor  $\pi/2$ . Although at this point the



**Figure 2.** The probability density  $|\psi(\mathbf{r}_{12})|^2$  of the lowest  $m = 0$  state (top) and the contour plots of the potential surface (bottom) for the QD with  $\omega_z/\omega_0 = 2$  and  $R_W = 10$  shown in the  $(\rho_{12}, z_{12})$ -plane for the cases: (a), (d)  $\omega_L/\omega_0 = 0$  ( $\omega_z/\Omega = 2$ ), (b), (e)  $\omega_L/\omega_0 = \omega_L^{\text{sph}}/\omega_0 = 1.732005$  ( $\omega_z/\Omega = 1$ ) and (c), (f)  $\omega_L/\omega_0 = 2.29129$  ( $\omega_z/\Omega = 0.8$ ).

3D system is far from the 2D model and from the 1D model and, as a consequence,  $R_\Omega^{(2D)}$  and  $R_\Omega^{(1D)}$  do not match smoothly, these two functions taken together give a qualitative picture of how the effective electron–electron interaction in a 3D QD changes with the magnetic field.

To get deep insight into this transition, we calculate the probability density  $|\psi(\mathbf{r}_{12})|^2$  and potential surfaces for various values of the magnetic field (see figure 2). Since the symmetry is exact for any strength of the electron–electron interaction at the transition point, in order to illuminate the effect, we use  $R_W = 10$ . For the magnetic field  $\omega_L < \omega_L^{\text{sph}}$ , the density maximum is located in the  $(x_{12}, y_{12})$ -plane ( $z_{12} = 0$ , see figure 2(a)). For  $\omega_L > \omega_L^{\text{sph}}$ , however, there are two maxima located symmetrically along the  $z_{12}$ -axis ( $\rho_{12} = 0$ , see figure 2(c)). The analysis of the behaviour of the stationary point of the potential  $V = \frac{1}{2}\mu(\Omega^2\rho_{12}^2 + \omega_z^2z_{12}^2) + k/r_{12}$  as a function of the magnetic field provides the explanation. For  $\omega_L < \omega_L^{\text{sph}}$  ( $\Omega < \omega_z$ ), the stationary point  $\rho_{12} = \rho_0, z_{12} = 0$  is the minimum of the potential surface (see figure 2(d)). Here  $\rho_0 = (k/\mu\Omega^2)^{1/3}$  [31]. By increasing the magnetic field over the value  $B_{\text{sph}}$  ( $\Omega > \omega_z$ ), the stationary point transforms to the saddle point and two new minima appear, divided by a potential barrier (see figure 2(f)). In other words, for  $m = 0$  a bifurcation of the stationary point located at  $(\rho_0, 0)$  occurs at the value of magnetic field when  $\omega_L = \omega_L^{\text{sph}}$  (see figures 2(b) and (e)). In the domain  $\Omega > \omega_z$ , for  $m = 0$ , the minima are located at  $z_{12} = \pm z_0$  in the  $z_{12}$ -axis ( $\rho_{12} = 0$ ), where  $z_0 = (k/\mu\omega_z^2)^{1/3}$ .

Summarizing, we have shown that the 3D approach provides a consistent description of the shape-phase transition in excited states in two-electron QDs under the magnetic field. The entanglement of the lowest state with  $m = 0$ , being first a decreasing function of the magnetic field, starts to increase after the transition point with the increase of the magnetic field. This behaviour is understood as the transition from the lateral to the vertical localization of the two-electron probability density for this state in the QD.

## Acknowledgments

This work is partly supported by RFBR grant no. 11-02-00086 (Russia), Project 171020 of Ministry of Education and Science of Serbia, Spanish MICINN grant no FIS2008-00781 and Project FQM-2445 of the Junta de Andalucía (Spain).

## References

- [1] Tichy M, Mintert F and Buchleitner A 2011 *J. Phys. B: At. Mol. Opt. Phys.* **44** 192001
- [2] Dehesa J S, Koga T, Yáñez R J, Plastino A R and Esquivel R O 2012 *J. Phys. B: At. Mol. Opt. Phys.* **45** 015504
- [3] Majtey A P, Plastino A R and Dehesa J S 2012 *J. Phys. A: Math. Theor.* **45** 115309
- [4] Esquivel R O et al 2011 *J. Phys. B: At. Mol. Opt. Phys.* **44** 175101
- [5] Carlier F, Mandilara A and Sarfati A 2007 *J. Phys. B: At. Mol. Opt. Phys.* **40** S199
- [6] Osenda O and Serra P 2008 *J. Phys. B: At. Mol. Opt. Phys.* **41** 065502
- [7] Bouvrie P A, Majtey A P, Plastino A R, Sanchez-Moreno P and Dehesa J S 2012 *Eur. Phys. J. D* **66** 15
- [8] Coe J P, Sudbery A and D' Amico I 2008 *Phys. Rev. B* **77** 205122
- [9] Pipek J and Nagy I 2009 *Phys. Rev. A* **79** 052501
- [10] Yáñez R J, Plastino A R and Dehesa J S 2010 *Eur. Phys. J. D* **56** 141
- [11] Kościak P and Okopińska A 2010 *Phys. Lett. A* **374** 3841
- [12] Laguna H G and Sagar R P 2011 *Phys. Rev. A* **84** 012502
- [13] Silva-Valencia J and Souza A M C 2012 *Phys. Rev. A* **85** 033612
- [14] Souza A M C and Almeida F A G 2009 *Phys. Rev. A* **80** 052337
- [15] Naudts J and Verhulst T 2007 *Phys. Rev. A* **75** 062104
- [16] Amico L, Fazio R, Osterloh A and Vedral V 2008 *Rev. Mod. Phys.* **80** 517
- [17] Sachdev S 2011 *Quantum Phase Transitions* 2nd edn (Cambridge: Cambridge University Press)
- [18] Reimann S M and Manninen M 2002 *Rev. Mod. Phys.* **74** 1283
- [19] Kais S, Herschbach D R and Levine R D 1989 *J. Chem. Phys.* **91** 7791
- [20] Taut M 1993 *Phys. Rev. A* **48** 3561
- [21] Taut M 1994 *J. Phys. A: Math. Gen.* **27** 1045
- [22] Nazmitdinov R G 2009 *Phys. Part. Nucl.* **40** 71
- [23] Kohn W 1961 *Phys. Rev.* **123** 1242
- [24] Fock V 1928 *Z. Phys.* **47** 446
- [25] Darwin C G 1930 *Proc. Camb. Phil. Soc.* **27** 86
- [26] Wagner M, Merkt U and Chaplik A V 1992 *Phys. Rev. B* **45** 1951
- [27] Nazmitdinov R G and Simonović N S 2007 *Phys. Rev. B* **76** 193306
- [28] Nazmitdinov R G, Simonović N S and Rost J M 2002 *Phys. Rev. B* **65** 155307
- [29] Simonović N S and Nazmitdinov R G 2003 *Phys. Rev. B* **67** 041305
- [30] Wojs A, Hawrylak P, Fafard S and Jacak L 1996 *Phys. Rev. B* **54** 5604
- [31] Coleman A and Yukalov V 2000 *Reduced Density Matrices* (Berlin: Springer)
- [32] Buscemi F, Bordone P and Bertoni A 2007 *Phys. Rev. A* **75** 032301
- [33] Simonović N S and Nazmitdinov R G 2008 *Phys. Rev. A* **78** 032115
- [34] Puente A, Serra L and Nazmitdinov R G 2004 *Phys. Rev. B* **69** 125315